S-Adenosyl-L-methionine-Dependent Methyl Transfer: Observable Precatalytic Intermediates during DNA Cytosine Methylation†

Ben Youngblood,‡ Fa-Kuen Shieh,§ Fabian Buller,§ Tim Bullock,§ and Norbert O. Reich*,‡,§

Department of Chemistry and Biochemistry and Program in Biomolecular Science and Engineering, University of California, Santa Barbara, California 93106-9510

Received March 28, 2007; Revised Manuscript Received May 26, 2007

ABSTRACT: *S*-Adenosyl-L-methionine- (AdoMet-) dependent methyltransferases are widespread, play critical roles in diverse biological pathways, and are antibiotic and cancer drug targets. Presently missing from our understanding of any AdoMet-dependent methyl-transfer reaction is a high-resolution structure of a precatalytic enzyme/AdoMet/DNA complex. The catalytic mechanism of DNA cytosine methylation was studied by structurally and functionally characterizing several active site mutants of the bacterial enzyme M.HhaI. The 2.64 Å resolution protein/DNA/AdoMet structure of the inactive C81A M.HhaI mutant suggests that active site water, a ∼13° tilt of the target base toward the active site nucleophile, and the presence or absence of the cofactor methylsulfonium are coupled via a hydrogen-bonding network involving Tyr167. The active site in the mutant complex is assembled to optimally align the pyrimidine for nucleophilic attack and subsequent methyl transfer, consistent with previous molecular dynamics ab initio and quantum mechanics/molecular mechanics calculations. The mutant/DNA/AdoHcy structure (2.88 Å resolution) provides a direct comparison to the postcatalytic complex. A third C81A ternary structure (2.22 Å resolution) reveals hydrolysis of AdoMet to adenosine in the active site, further validating the coupling between the methionine portion of AdoMet and ultimately validating the structural observation of a prechemistry/postchemistry water network. Disruption of this hydrogen-bonding network by a Tyr167 to Phe167 mutation does not alter the kinetics of nucleophilic attack or methyl transfer. However, the Y167F mutant shows detectable changes in k_{cat}, caused by the perturbed kinetics of AdoHcy release. These results provide a basis for including an extensive hydrogen-bonding network in controlling the rate-limiting product release steps during cytosine methylation.

DNA methyltransferases catalyze the epigenetic modification of cytosine (C-5 and N-4) and adenine (N-6) methylation (*1*, *2*), which play important roles in many cellular events including DNA replication, defense against phage invasion, mismatch repair, and gene regulation. The human homologues DNMT1, DNMT2, DNMT3a, and DNMT3b modify DNA at cytosine C-5 exclusively and are essential for gene regulation, genetic imprinting, and host defense mechanisms (*3*). Because of their involvement in bacterial virulence and tumorigenesis, the bacterial and human enzymes are targets of antibiotic and cancer therapeutic drug development efforts, respectively (*4*−*6*).

The first ternary crystal structure of an *S*-adenosyl-L-methionine- (AdoMet-)[1] dependent methyltransferase was of the M.HhaI/DNA/*S*-adenosyl-L-homocysteine (AdoHcy) complex (*7*). This structure provided new insights into the catalytic mechanism, in particular the extrahelical repositioning of the target base into the active site of the enzyme adjacent to the bound product, AdoHcy (*7*). The resultant proximal positioning of the AdoHcy, and by implication, AdoMet methylsulfonium, to the C-5 of the cytosine target base provides an ideal trajectory and distance for the methyl-transfer reaction to occur (*7*) (Scheme 1). Our understanding of the chemical mechanism of DNA cytosine methylation and AdoMet-dependent methylation in general includes the extensive structural and kinetic studies of M.HhaI (Scheme 1) (*7*−*21*).

The extrahelical repositioning of the target base and rearrangement of a flexible protein loop form part of an induced fit mechanism (panel A vs panel C of Figure 1). The loop relocation correctly positions active site residues such as Cys81 which forms the covalent intermediate. Methylation is generally thought to proceed through an S_N2 mechanism (*11*), initiated by nucleophilic attack from the conserved cysteine residue 81 which resides in the flexible loop (Scheme 1) (*10*). Some degree of protonation of the cytosine via one or more active site residues (e.g., Glu119, Arg165, Arg163) or water molecule was previously proposed as an essential step to activate the ring for nucleophilic attack (*2*, *16*). We recently confirmed the importance of both Arg165 and Glu119 in the catalytic mechanism (*22*) (Shieh and Reich, submitted). Following protonation, the methyl-

† This work was supported by NSF Grant MCB-9983125 and NIH Grant RO1GM053763-08A2. This work was also partially funded through a scholarship from the Dr. Peter Schaefer Program for Sustainable Development, awarded to F.B.

* To whom correspondence should be addressed: e-mail, reich@chem.ucsb.edu; tel, 805-893-8368; fax, 805-893-4120.

‡ Program in Biomolecular Science and Engineering, University of California.

§ Department of Chemistry and Biochemistry, University of California.

[1] Abbreviations: AdoMet, *S*-adenosyl-L-methionine; AdoHcy, *S*-adenosyl-L-homocysteine; NAC, near attack conformer.

10.1021/bi7005948 CCC: $37.00
Published on Web 07/07/2007

Scheme 1: Proposed Catalytic Mechanism of DNA Methylation by M.HhaI[a]

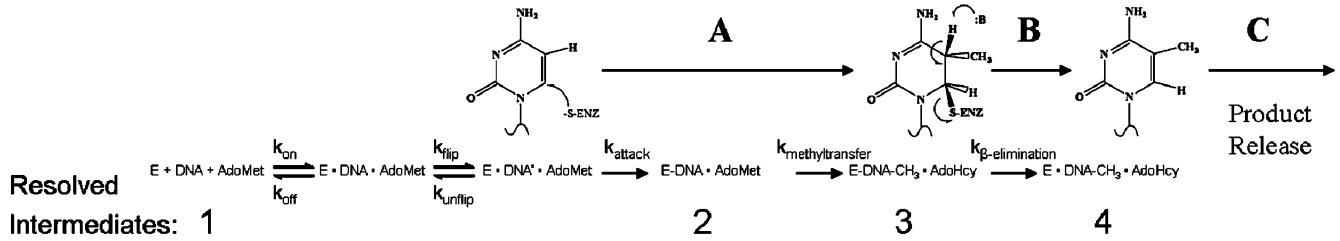

[a] *E* = enzyme, DNA = DNA substrate, DNA* = extrahelical target base, DNA-CH_3 = methylated DNA, AdoMet = *S*-adenosyl-L-methionine, and AdoHcy = *S*-adenosyl-L-homocysteine. Numbers below intermediates have the following correspondence to representative structures available in the PDB: **1**, 1HMY and 2HMY; **2**, 6MHT; **3**, 1MHT; **4**, 3MHT, 4MHT, 5MHT, 7MHT, 8MHT, 9MHT, and 10MH. [Scheme 1 adapted from Sharma et al. (*36*).] Steps A, B, and C represent transitions that may be influenced by an active site water.

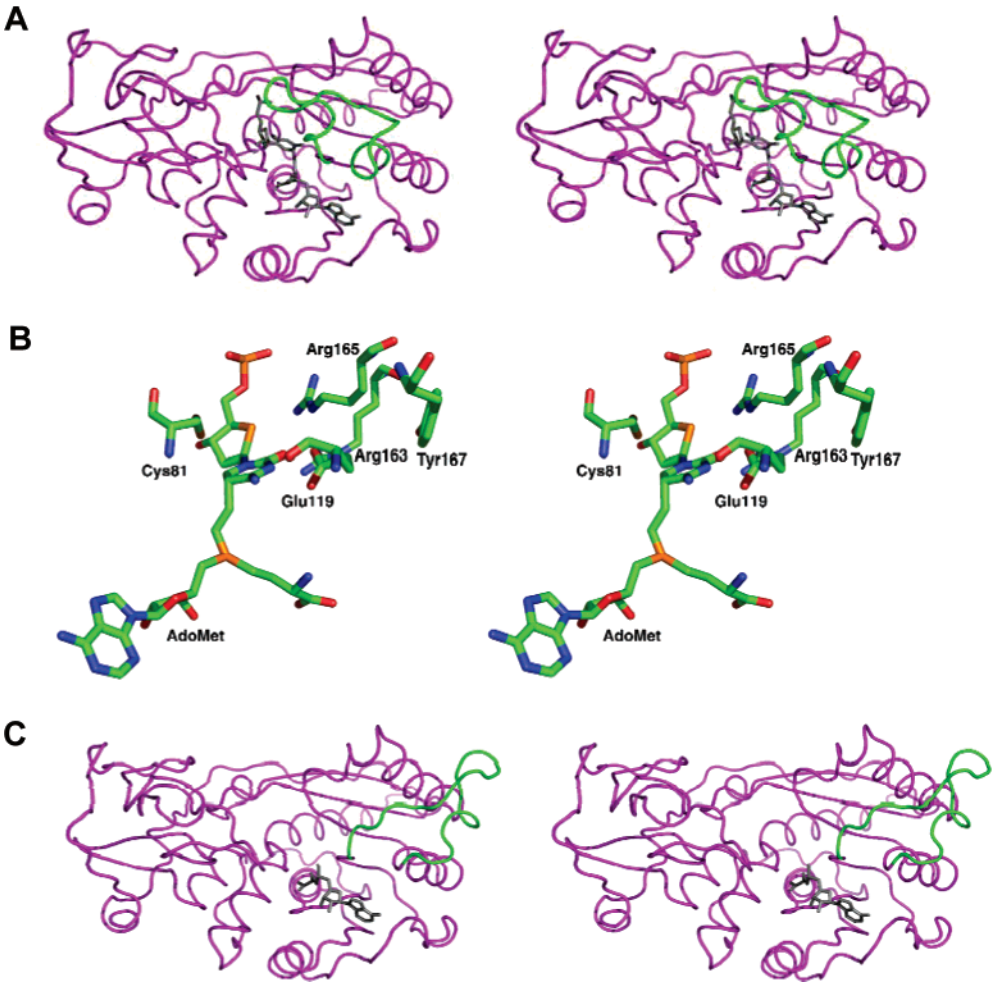

FIGURE 1: Ternary crystal structures of M.HhaI. (A) M.HhaI in complex with AdoMet and fluorinated DNA which forms a covalent linkage between the cofactor and DNA base. All DNA bases except for the fluorinated cytosine are omitted for clarity. The catalytic flexible loop (green; residues 80−99) is in the "closed" position. PDB code 6MHT. (B) Stereoview of the ternary covalent complex active site. (C) M.HhaI bound to AdoMet and nonspecific DNA. The catalytic flexible loop (green; residues 80−99) is in the "open" position causing Cys81 to be positioned outside of the enzyme active site. PDB code 2HMY. No density for DNA is observed, most likely due to an inconsistent repeat of the DNA throughout the crystal lattice (X. Cheng, personal communication).

sulfonium of AdoMet is then attacked by the C-5 position of the target base, leading to methyl transfer and β-elimination, which regenerates the enzyme (Scheme 1) (*10*, *19*, *23*). A recent quantum mechanical/molecular mechanics analysis of the M.HhaI mechanism suggests that the methyl-transfer reaction is actually concerted and the deprotonation step leading to nucleophile activation arises from hydroxide in the active site rather than an active site residue (*24*).

Molecular dynamics simulations of M.HhaI have implicated several active site water molecules as being catalytically important (*7*, *12*, *16*). Also, simulations have suggested that the target base tilts up to Cys81 to form a near attack conformer, and this change is coupled to the movement of several active site water molecules (*16*). These and other simulations are based on extensive cocrystal structures of M.HhaI bound to various DNA molecules, all of which involve the product *S*-adenosyl-L-homocysteine (AdoHcy). To date, 21 structures of mutant and WT M.HhaI bound to various cofactors and substrates have been published (*7*, *18*, *22*, *25*−*33*). A key unresolved intermediate, as shown in

Scheme 1, is of the enzyme bound to unmethylated DNA and AdoMet (prechemistry). To date, the majority of the structures involve the cofactor analogue AdoHcy, which is the product of AdoMet after the methyl-transfer step has occurred (postchemistry). Thus, structural inspection of the prechemistry active site of M.HhaI may provide insights into the mechanism of methyl transfer. Here we report three new crystal structures of the M.HhaI mutant in which the active site Cys81 was converted to an alanine, which provide mechanistic insights not previously available.

MATERIALS AND METHODS

Mutant Design. Cys81 was mutated to an alanine to remove the catalytic thiol group and to reduce steric hindrance. Also, C81A was created on the basis of prior observations that C81G retained tight DNA affinity yet had no detectable catalytic activity (*23*). Tyr167 was chosen for mutation based on the observed hydrogen bond from the hydroxyl group of Tyr167 to the mobile water present in the newly solved C81A crystal structures.

DNA Affinity. Two dsDNA substrates, Abox and AMbox,

Abox: 5′-GGGAATTCATGGCGCAGTGGGTGGATCCAG-3′

3′-CCCTTAAGTACCGCGTCACCCACCTAGGTC-5′

AMbox: 5′-GGGAATTCATGGCGCAGTGGGTGGATCCAG-3′

3′-CCCTTAAGTACCGC^{Me}GTCACCCACCTAGGTC-5′

were used for the DNA affinity studies as previously reported (*8*). Electrophoretic gel mobility shift assays were performed with 10 pM ^{32}P-labeled DNA and increasing enzyme concentrations. Radiolabeled DNA and enzyme were mixed in methylation reaction buffer (100 mM Tris-HCl, pH 8.0, 10 mM EDTA, 10 mM DTT, 0.2 mg/mL bovine serum albumin) with 10 μM *S*-adenosyl-L-homocysteine (AdoHcy). Densitometry of shifted bands was analyzed on a Storm 840 phosphorimager measured with the program Imagequant. Data were fit to a rectangular hyperbola using the program SigmaPlot.

Burst Analysis (k_{cat}). Time course assays were performed at 37 °C under saturating substrate concentrations. Reactions were carried out in methylation reaction buffer in the presence of 2.8 μM [*methyl*-^{3}H]AdoMet/unlabeled AdoMet mix. The reactions were initiated by the addition of either DNA or enzyme to preincubated mixtures, to give a final DNA concentration of 5 μM and enzyme concentration of 20 nM. Values for k_{cat} were obtained by dividing the slope of the time course assay by the concentration of the enzyme. Active site titration was used to calculate the concentration of WT and Y167F M.HhaI; for validation, this concentration was then compared to an absorbance reading at 280 nm.

Single-Turnover Analysis (k_{chem} and $k_{inactivation}$). Time course assays were performed at 4 °C. The reactions were initiated by adding enzyme to the mixture of methylation reaction buffer, DNA substrate, and [*methyl*-^{3}H]AdoMet (5.5 μM). Final DNA concentration was 500 nM, and final enzyme concentration was 4 μM. The reaction was quenched at 35 min with sodium dodecyl sulfate and spotted on DE81 filter paper. Values for k_{chem} were obtained by fitting the data to a single exponential equation. For $k_{inactivation}$ studies FMbox DNA was used, which is the same as AMbox but contains a fluorinated cytosine on the top strand at the position of the target cytosine, which traps the enzyme−DNA covalent intermediate. FMbox DNA single-turnover assays were performed with AdoMet (5.5 μM) and enzyme (750 nM) in protein dilution buffer incubated at 37 °C. Reactions were initiated by FMbox DNA addition (300 nM). Time points taken at 10, 20, 40, 60, 90, 120, and 150 min were spotted on DE-81 filters. Filter papers were washed with phosphate buffer; then tritium incorporation was measured using a Beckman Coulter LS6500 liquid scintillation counter.

Cofactor Binding. A Perkin-Elmer LS50B luminescence spectrometer was used for fluorescence measurements as described previously (*17*). Excitation and emission slit widths were 5.0 mm. A xenon lamp was used at an excitation wavelength of 280 nm. Emission spectra were recorded from 320 to 400 nm from a 1 cm length quartz cuvette at 25 °C containing enzyme (1 μM), 100 mM Tris, pH 8.0, 10 mM EDTA, and 10 mM dithiothreitol. Spectra were recorded as the *S*-adenosyl-L-methionine (AdoMet) concentration was varied from 0 to 176 μM. The K_D for AdoMet was measured by the loss of fluorescence intensity from the tryptophan in the AdoMet binding pocket (*17*). The observed tryptophan fluorescence after AdoMet addition was subtracted from the initial intensity, F_o. $F_o - F$ versus AdoMet concentration was plotted using the program SigmaPlot, with the curve fit to a rectangular hyperbola.

Steady-State Kinetic Analysis. The constant K_M^{AdoMet} was measured by a titration of [*methyl*-^{3}H]AdoMet from 50 nM to 3.2 μM, with 5 μM Abox DNA and 200 pM enzyme. The reaction was carried out in methylation reaction buffer for 15 min. The rate of methyl transfer was calculated by spotting the reaction solution on DE81 filter paper and counting the tritium incorporation with a liquid scintillation counter. Values for K_M^{AdoMet} were obtained by fitting the data to a rectangular hyperbola using the program SigmaPlot.

Crystallization. Complementary oligodeoxynucleotides were purchased from Midlands DNA (Midlands, TX). The DNA substrate 5′-TGATAGCGCTATC-3′ was synthesized for cocrystallization trials by standard methods and purified on a Rainin Pure DNA HPLC column developed in a gradient of TEAA/acetonitrile. The DNA was collected manually, lyophilized, and stored as dry pellets at −20 °C until ready for use, when it was brought to a concentration of 10 mg/mL in 50 mM Tris (pH = 7.5)/1 mM EDTA. The protein at a final concentration of 7 mg/mL was mixed with DNA and *S*-adenosyl-L-homocysteine (AdoHcy) or AdoMet. Cocrystals were grown by hanging drop vapor diffusion at 17 °C; 1.5 μL of enzyme C81A M.HhaI (240 μM), DNA (480 μM), and AdoHcy or AdoMet (960 μM) was mixed with 1.5 μL of crystallization solution (100 mM sodium citrate buffer, pH 5.5 or 6.0, 45−55% 3.5 M ammonium sulfate) and placed over a well containing the crystallization solution. Cocrystals with dimensions of 150 μm × 150 μm × 300 μm formed within 10−48 h. Prior to X-ray data collection the cocrystals were transferred into a cryoprotectant solution (100 mM sodium citrate buffer, pH 5.5 or 6.0, 30% glycerol) and flash frozen in liquid nitrogen.

Data Collection and Structure Determination. C81A M.HhaI-AdoHcy-DNA cocrystal X-ray data were collected in-house using a rotating copper anode (Nonius) with an

Table 1: Kinetic and Thermodynamic Constants for WT and Mutant M.HhaI Enzymes

enzyme	k_{cat} (s^{-1})	K_D^{DNA} (nM)	K_D^{AdoMet} (μM)	K_M^{AdoMet} (nM)	$k_{inactivation}$ (min^{-1})	k_{chem} (s^{-1})[a]
WT	0.085 ± 0.0089	0.190 ± 0.050	12 ± 2.1	550 ± 59	0.019 ± 0.0045	0.018 ± 0.0024
C81A	$<1 \times 10^{-7}$	0.160 ± 0.050	2.9 ± 0.30	nd[b]	nd	nd
Y167F	0.016 ± 0.0032	0.110 ± 0.034	2.9 ± 0.17	140 ± 28	0.022 ± 0.0013	0.018 ± 0.0019

[a] k_{chem} was measured at 4 °C. [b] nd = not determined.

image plate detector (Mar Research) at 100 K. Integration, scaling, and merging of data were carried out with MOSFLM. The known structure of WT M.HhaI in complex with the DNA and cofactor AdoHcy (PDB file 3MHT) was used as the initial model with the Cys81 side chain replaced with an alanine side chain. The mutant was isomorphous with the WT enzyme allowing direct phasing by Fourier synthesis. Structure determination consisted of several rounds of model building with the computer program O (*46*) iterated with individual *B*-factor and simulated annealing refinement using CNS (*47*) (Table 3). The X-ray diffraction amplitudes for the C81A M.HhaI-AdoMet-DNA cocrystals were collected using a Rigaku Raxis IV^{++} area detector (MAR) mounted on a Rigaku RU-300B rotating anode generator at Amgen Inc., Thousand Oaks, CA. The exposure time was 10 min every 1° rotation at 50 kV, 100 mA with a wavelength of 1.541 Å at 100 K. Ternary structure reflection indexes, integration, scaling, and merging of data were carried out with HKL2000 software.

Restacking Kinetics. Stopped-flow data were collected with an Applied Photophysics SX.18MV stopped-flow reaction analyzer outfitted with a single channel emission photomultiplier tube. An excitation wavelength of 310 nm and a cutoff filter of 320 nm were used for data collection. The rate of extrahelical base restacking was measured by monitoring the dissociation of the preformed 2-aminopurine- (2AP-) containing DNA−enzyme complex. 2AP fluorescence is roughly 14-fold greater when extrahelical (*26*, *44*, *48*), and the loss of fluorescence was attributed to the restacking of the target base. A final concentration of 100 nM 2AP DNA, 100 nM enzyme, and 5 μM AdoMet was mixed with 5 μM unlabeled cognate competitor DNA. The fluorescence data were fit to a double exponential equation using the program Sigma Plot. The 2AP base substitutes for the target cytosine in the hemimethylated duplex substrate. Prior characterization of M.HhaI base flipping using 2AP also reports observing two distinct phases attributed to two steps in the base flipping process (*44*, *45*).

RESULTS AND DISCUSSION

Functional Characterization of the Active Site Nucleophile. The Cys81 to Ala81 mutant was designed to cause the least perturbing change in the enzyme structure while removing the active site nucleophile, thus allowing the study of the enzyme bound to both substrates. C81A M.HhaI lacks detectable catalytic activity[2] yet has greater than WT affinity for DNA and cofactor AdoMet (Table 1), similar to other previously characterized Cys81 mutants (*23*). This provides a basis for obtaining the C81A M.HhaI cocrystal structure with the biologically relevant cofactor *S*-adenosyl-L-methionine (AdoMet). Two previous M.HhaI structures have included both AdoMet and either modified or nonspecific DNA. The modified DNA substrate contained a 4′-thio-2′-deoxycytidine in place of the target base (*14*) and yielded a partially methylated DNA target base (Figure 1A,B). The structure containing nonspecific DNA (*30*) has no electron density for the DNA (Figure 1C). Importantly, these two structures do not provide critical information about the active site poised for catalysis. Similarly, the ternary structures of other AdoMet-dependent enzymes have relied exclusively on the use of AdoHcy or substrate analogues.

Table 2: Crystallographic Parameters for C81A M.HhaI AdoMet, AdoMet^{hydrolyzed}, and AdoHcy Ternary Structures

	C81A-AdoHcy	C81A-AdoMet	C81A-AdoMet^{hydroyzed}
Data Collection			
resolution limit (Å)	2.88	2.64	2.25
wavelength (Å)	1.541	1.541	1.541
measurements	140944	140783	874999
unique reflections	14120	21247	29064
space group	*R*32	*R*32	*R*32
unit cell dimension			
$a = b$ (Å)	98.43	98.57	98.48
c (Å)	323.61	322.91	322.49
redundancy[a]	3.5 (3.6)	3.2 (2.9)	11 (10.9)
completeness (%)[a]	99.9 (99.9)	99.3 (100)	97.8 (96.4)
$\langle I/\sigma(I)\rangle$[a]	6.3 (2.0)	6.6 (2.1)	6.1 (5.7)
R_{merge} (%)[a,b]	9.0 (35.4)	7.9 (34.8)	4.7 (33.5)
Refinement			
R_{factor} (%)[c]	22.42	22.48	25.23
R_{free} (%)[d]	28.17	27.88	28.85
rmsd from std geometry			
bond length (Å)	0.0074	0.0071	0.0068
bond angles (deg)	1.52	1.35	1.35
overall *B*-factor	37.17	33.62	35.47
no. of waters	54	83	94

[a] Values in parentheses are for the highest resolution data shell. [b] $R_{merge} = \sum|I - \langle I\rangle|/\sum\langle I\rangle$, where I is the observed intensity. [c] $R_{factor} = \sum|F_o - F_c|/\sum F_o$. [d] R_{free} is as for R_{factor} but calculated using a 10% test set of reflections excluded from the refinement.

Structural Analysis of C81A M.HhaI-DNA-AdoMet, C81A M.HhaI-DNA-AdoMet^{hydrolyzed}, and C81A M.HhaI-DNA-AdoHcy. The C81A M.HhaI-DNA-AdoMet ternary crystal structure (C81A-AdoMet) was solved in order to examine the prechemistry positioning of active site residues, target base, cofactor, and water molecules. The C81A-AdoMet-DNA crystal diffracted to 2.64 Å (Table 2). The M.HhaI-AdoHcy-DNA cocrystal structure (3MHT) with the Cys81 mutated to Ala was used as the initial phasing model. All relevant values for each data set are reported in Table 2. A second ternary crystal structure of the C81A M.HhaI mutant containing DNA and AdoHcy was solved so that the C81A M.HhaI structures could be compared with previous WT M.HhaI structures solved with AdoHcy. The C81A-AdoHcy-DNA crystal diffracted to 2.88 Å (Table 2). A third C81A ternary structure was solved with AdoMet, in which data collection was done approximately 1 month after the crystal was formed (AdoMet^{hydrolyzed}). Our intent was to observe

[2] Catalytic activity decreased $>10^6$-fold compared to WT M.HhaI and thus is not measurable (*8*).

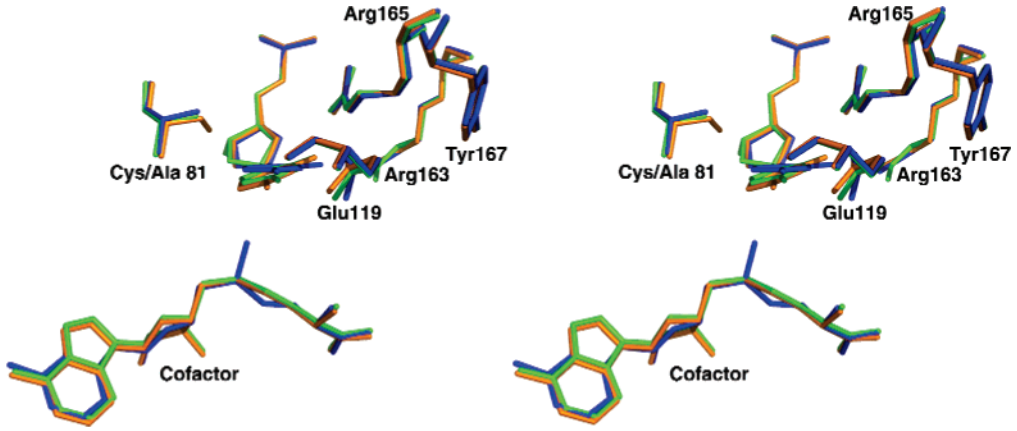

FIGURE 2: Stereoview of active site residues from superimposed structures of C81A M.HhaI-DNA-AdoHcy (green), C81A M.HhaI-DNA-AdoMet (blue), and WT-DNA-AdoHcy (orange). Superimposed DNA molecules are colored orange. Superimposed cofactors are colored gray. The root-mean-square deviation (rmsd) between the backbone atoms for all three enzymes is <0.3 Å. Differences between target base positioning may also be observed in the difference maps of Figure 3.

complete or partial methyl transfer from AdoMet to the DNA within the crystal. The C81A-AdoMet^{hydrolyzed}-DNA crystal diffracted to 2.25 Å (Table 2). The root-mean-square deviation (rmsd) for each structure compared to a recently solved high-resolution WT structure (PDB ID 2HR1) (*22*) is less than 0.30 Å, which is within the coordinate error; thus the global structures are identical to the WT enzyme (Figure 1C). Both large and small domains of the three C81A M.HhaI structures are brought within van der Waals contact of the DNA substrate forming specific interactions with the phosphate backbone and bases. In contrast, the M.HhaI ternary structure containing nonspecific DNA (Figure 1C) shows the small domain ~2 Å extended away from the DNA backbone. All three C81A M.HhaI structures contain the flexible catalytic loop (residues 80−99) in the closed conformation (Figure 1C) as observed with the previously reported covalent complex structure (*14*) (Figure 1A,B). Because the catalytic loop in all three C81A M.HhaI structures is in the closed conformation, we suggest that these structures represent either intermediates poised for methyl transfer (AdoMet ternary complex) or an intermediate following the chemistry step (AdoHcy ternary complex) (Figures 2, 3, and 4). Additionally, since the AdoMet in the C81A M.HhaI structure is in the primed orientation as previously described by O'Gara et al. (*30*) and methyl transfer has not yet occurred (Figure 3), this intermediate represents the prechemistry intermediate.

Cofactor and Active Site Water Positioning Are Coupled. All three C81A crystal structures [along with a previously reported 1.9 Å WT-DNA-AdoHcy structure (PDB ID 2HR1) (*22*)] were found to be isomorphous with one another, thus allowing for an $F_o - F_o$ analysis (calculates differences between Fourier synthesized electron density maps of two different crystallographic data sets) which can reveal subtle difference between each structure. The high-resolution (1.9 Å) WT M.HhaI structure (PDB ID 2HR1) (*22*) was used in the $F_o - F_o$ analysis instead of the original lower resolution WT structure (*7*), used for the initial phasing, so that more confidence could be placed in the conclusions made about small differences of the active site. The only significant structural differences revealed by the $F_o - F_o$ analysis between the C81A/AdoMet−C81A/AdoHcy structures are localized to the active site (Figure 3). The difference map between these two structures reveals a large, previously unidentified density in the C81A-AdoMet-DNA structure that does not correspond to any amino acid (Figure 3A, blue density contoured at ~5.0σ between Glu119 and Tyr167). There were no metals present in the crystallization conditions, and this new density is within an ideal hydrogen-bonding distance to the hydroxyl of Tyr167. We suggest that this new electron density is a water molecule, since it has the correct dimensionality. In addition, the difference map between C81A-AdoMet-DNA and WT-AdoHcy-DNA also reveals the same density for a single water in this newly identified position (Figure 3A, green density contoured at ~5.0σ between Glu119 and Tyr167). Because of the high contouring level in both difference $F_o - F_c$ maps and the low *B*-factor values (Table 3), we are confident that this water at this new position is real.

In the $F_o - F_o$ map between C81A-AdoMet-DNA and WT-AdoHcy-DNA, the negatively contoured density reveals the expected density for the sulfur group of Cys81 in the WT structure (Figure 3, red density above C5 position of target cytosine). Both difference maps clearly show density surrounding the methyl group of the AdoMet which is missing in both WT-DNA-AdoHcy and C81A-DNA-AdoHcy structures (Figure 3A). The tilt of the target base of 13.6° toward Ala81 (determined by measuring the difference between the C-5 atoms of the target cytosine with the N-3 of the cytosine as the center atom for the angle measurement) is observed with the negative density of both difference maps (Figure 3B, blue and green density below target cytosine). The observed change in the target base tilt is the first structurally resolved evidence that indeed the base tilts toward the nucleophilic cysteine prior to the chemistry event.

The prechemistry active site of M.HhaI reveals insights into the chemical mechanism for methyl transfer. The tilt of the target base may result from two possibilities: (1) The methyl-transfer mechanism relies on the subtle repositioning of the cytosine to enhance nucleophilic attack. (2) Removal of the thiol in the C81A mutation causes the target base to compensate by rotating in the direction of the missing thiol. The active sites in the three ternary structures retain the flipped out target base appropriately positioned for nucleophilic attack by the thiol. The difference in the tilt of the

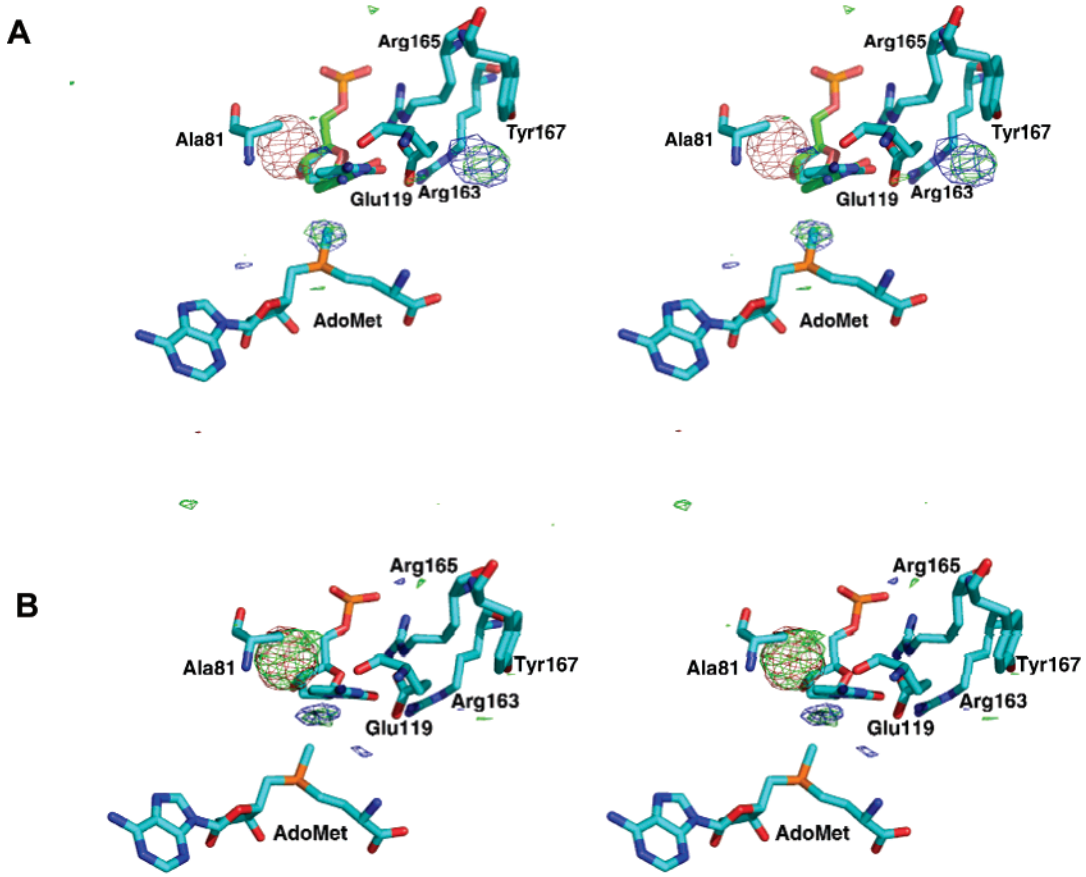

FIGURE 3: Electron density of $F_o - F_o$ maps: C81A-DNA-AdoMet minus WT-DNA-AdoHcy, C81A-DNA-AdoMet minus C81A-DNA-AdoHcy, and WT-DNA-AdoHcy minus C81A-DNA-AdoHcy. (A) Positive density (blue and green meshes contoured at ~5.0σ) showing where the methyl group on the cofactor appears with C81A-DNA-AdoMet minus WT-DNA-AdoHcy and C81A-DNA-AdoMet minus C81A-DNA-AdoHcy. Density from the $F_o - F_o$ difference map appears at the C81A mutation for WT-DNA-AdoHcy minus C81A-DNA-AdoHcy. The target base from a high-resolution WT structure is superimposed with the target base in the mutant structure. (B) Negative density (red mesh contoured at ~5.0σ) showing the base moves away from the methyl group for C81A-DNA-AdoMet minus WT-DNA-AdoHcy and C81A-DNA-AdoMet minus C81A-DNA-AdoHcy.

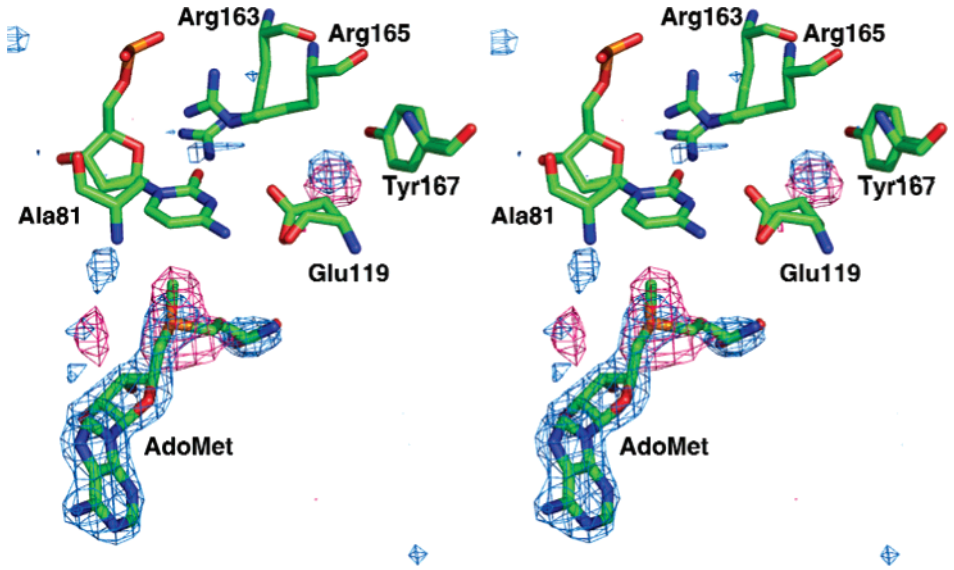

FIGURE 4: Electron density maps showing cofactor hydrolysis and water movement. Blue electron density (contour at 1.0σ) = $F_o - F_c$ of a calculated Fourier transform without coordinates for the cofactor. Red electron density (contour at 1.0σ) = $F_o - F_o$ of C81A-DNA-AdoMet^{hydrolyzed} crystal reflections minus C81A-DNA-AdoMet crystal reflections. A backbone for the *S*-adenosyl-L-methionine was added back in after calculation of the $F_o - F_c$.

base between the C81A-DNA-AdoMet and C81A-DNA-AdoHcy structures (Figure 3B) suggests that the change arises from the cofactor methyl group and is not an artifact of the C81A mutation. We suggest that the 13° tilt of the target base most likely facilitates the approach to the transition state of the enzyme−DNA covalent adduct.

Table 3: Active Site Water *B*-Factor Comparison[a]

H_2O position	C81A-AdoHcy	C81A-AdoMet	C81A-AdoMet^{hydrolyzed}	WT-AdoHcy
average of all observable H_2O (Å^2)	29.0 ± 8.12	29.4 ± 7.74	39.2 ± 5.85	33.2 ± 6.82
networked to Tyr167 (Å^2)	27.9 (−1.10)	11.8 (−17.6)	49.9 (+10.7)	25.24 (−8.00)[b]
networked to Gln82 (Å^2)	n.o.	24.9 (−4.50)	36.3 (−2.90)	24.5 (−8.70)

[a] Parentheses = difference from average water *B*-factor. Total number of water molecules: WT-AdoHcy = 164, C81A-AdoHcy = 54, C81A-AdoMet = 83, and C81A-AdoMet^{hydrolyzed} = 94. n.o. = not observed. Standard deviation for average of all H_2O is reported as ±. [b] Single water selected around Tyr167 in the WT structure.

Further, these structures support a mechanism in which the active site functions to limit the movement of the nucleophile, target base, and methyl donor (AdoMet), while retaining the proper trajectory for nucleophilic attack of the C-6 carbon of the target base by the thiol (*16*, *34*, *35*). Interestingly, the importance of the target base repositioning toward Cys81 to facilitate methyl transfer was previously suggested, based on molecular dynamics simulation (*16*). Further, the change in base tilt of ~13° that we observe is within the assigned trajectory for a near attack conformer (NAC), defined as a conformation of the enzyme and substrate that very closely resembles the transition state of a bond-breaking or -making step (*35*).

The active sites of several AdoMet-dependent enzymes have been proposed to involve a compressive transition state during methyl transfer (*16*, *36*−38). Importantly, the experimental evidence, largely based on kinetic isotope studies, is not in complete agreement with molecular dynamics predictions (*39*). Our observation that the target base is tilted toward the nucleophile in the prechemistry structure suggests that some type of compression may be occurring with M.HhaI. The NAC, as predicted by molecular dynamics (rotation of the target base about the C1′−N1 bond between the sugar and target base reducing the distance between the sulfhydryl group of Cys83 to the target base C6), supports the catalytic enhancement arising from substrate preorganization as opposed to stabilization of the transition state. The NAC concept does not preclude transition state stabilization as an enhancement factor. Simply stated, a substrate preorganization hypothesis predicts that entropically driven preorganization of the substrate increases the probability of sampling the transition state (*37*). Our thermodynamic measurements of mutant and WT M.HhaI K_D^{DNA} and K_D^{AdoMet} reveal that the affinities of the C81A M.HhaI prechemistry complex for the substrates are tighter than the corresponding WT M.HhaI affinities (Table 1). This indirectly suggests that intermediates **2**−**4** (Scheme 1) are not extensively populated during the normal methylation cycle.

The repositioning of an active site water was previously implicated to be important for the reaction catalyzed by M.HhaI (*16*). The water in the newly identified position that we observe in the prechemistry active site appears to be the starting position of a water observed to move toward the target base during the same molecular dynamics simulation that also predicts the tilt of the target base (*16*). Our work therefore supports the prior predictions that the tilt of the target base and water positioning in the active site of the enzyme are indeed part of the M.HhaI catalytic mechanism.

The observed loss of density for the water, which is hydrogen bonded to Tyr167 in the WT M.HhaI-DNA-AdoHcy and C81A M.HhaI-DNA-AdoHcy structures, suggests that the cofactor methyl group is coupled with the positioning of the active site water. C81A-AdoMet^{hydrolyzed}-DNA crystals were stored for 1 month at 17 °C in an attempt to observe catalysis and movement of the water. Diffraction data were collected, and the coordinates for the AdoMet molecule were excluded from the calculated $F_o - F_c$ map to reveal the electron density for the entire cofactor (Figure 4, blue density). Also, the calculated $F_o - F_c$ map reveals that the water near Tyr167 is in the prechemistry position as observed with the prior C81A-DNA-AdoMet structure (Figure 3A). Interestingly, a $F_o - F_o$ analysis between C81A-DNA-AdoMet minus C81A-DNA-AdoMet^{hydrolyzed} results in a loss of electron density corresponding to the methionine portion of the AdoMet cofactor (Figure 4, blue density). Thus, the only chemical modification occurring from the extended incubation of the crystals is the hydrolysis of the cofactor, consistent with the cofactor's susceptibility to hydrolysis (*40*). The concomitant loss of the active site water in the prechemistry position, as observed by loss of electron density in the $F_o - F_o$ analysis (Figure 4, blue density), suggests that the presence of the methionine portion of the cofactor is necessary for the prechemistry positioning of the active site water.

To provide a more quantitative analysis of the pre- and postchemistry water positioning, the *B*-factors for all waters were examined in each crystal structure. Table 3 reports the *B*-factors for the water hydrogen bonded to Tyr167 and, as a control, a different water in the active site hydrogen bonded to Gln82 [previously implicated to be important in catalysis by computer simulations (*16*)]. Individual *B*-factors for these two waters are within one standard deviation of the average *B*-factor of all waters in the entire crystal structure (difference from average value in parentheses), except for the Tyr167 hydrogen-bonded water in the C81A-DNA-AdoMet and C81A-DNA- AdoMet^{hydrolyzed} structures. The *B*-factor for this Tyr167 hydrogen-bonded water is significantly lower than the average *B*-factor (difference is 2.3-fold greater than the standard deviation) (Table 3). Furthermore, hydrolysis of the cofactor (C81A-DNA-AdoMet^{hydrolyzed}) results in the *B*-factor for this water increasing 1.8-fold above the standard deviation (Table 3). Hydrolysis of the AdoMet in the crystal lattice leads to the water hydrogen bonded to Tyr167 becoming less identifiable, hence the higher *B*-factor (Table 3). Since *B*-factors are a measure of thermal motion (*41*), these differences indicate that the hydrogen-bonded water is coupled to the presence of the methionine portion of AdoMet, specifically the methyl group, as observed with the difference maps of the C81A-DNA-AdoMet^{hydrolyzed} structure (Figure 4).

Disruption of the Water Bonding Network by Mutating Tyr167 to Phe167. On the basis of our observation that placement of the water hydrogen bonded to Tyr167 is coupled to the occupancy of AdoMet in the cofactor binding

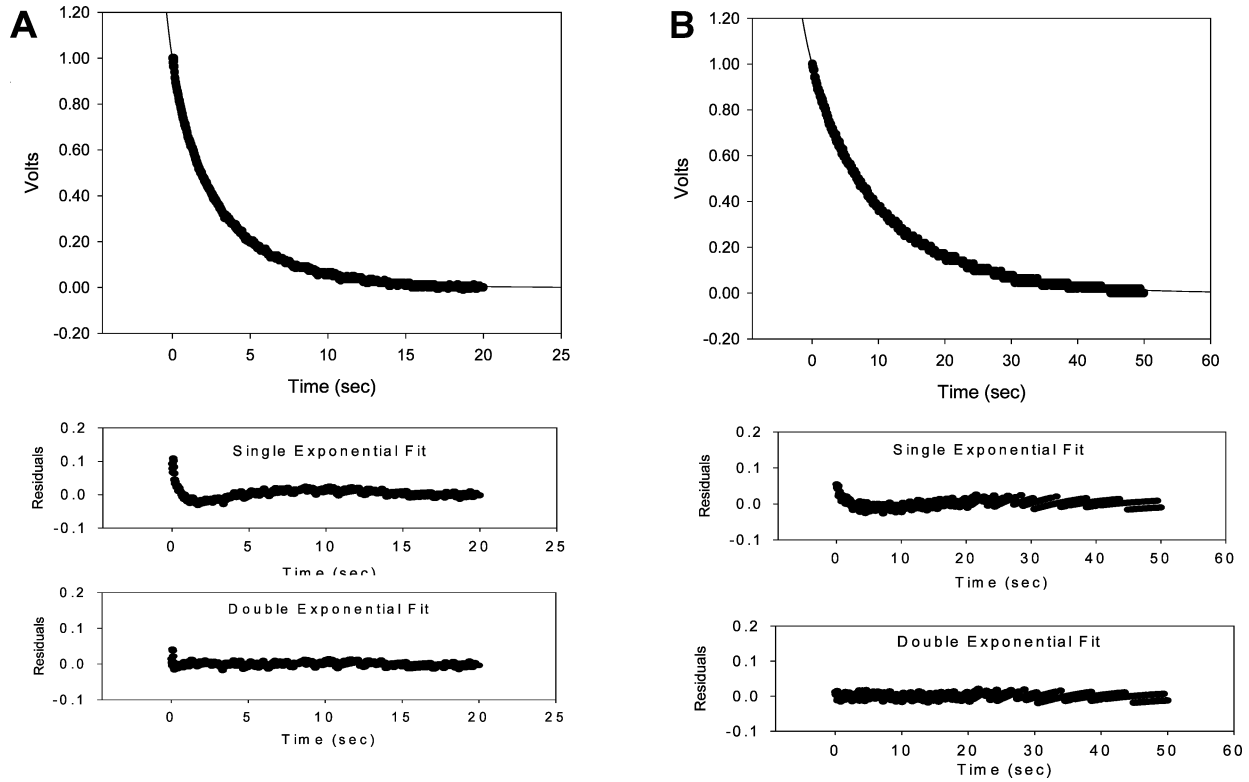

FIGURE 5: Y167F has altered forward and reverse base stacking kinetics as monitored by 2AP fluorescence: (A) WT and (B) Y167F. Restacking rates were determined by mixing the preformed M.HhaI-2AP DNA-AdoHcy complex with the 50-fold nonfluorescent competitor cognate DNA. Restacking rates were best fit to a double exponential equation (solid line through the data points), with two given rates and amplitudes reported for each enzyme. Single and double exponential fits are shown below the corresponding data set. WT rate 1 = 1.1 s^{-1}, amplitude 1 = 23%, rate 2 = 0.26 s^{-1}, amplitude 2 = 77%. Y167F rate 1 = 0.38 s^{-1}, amplitude 1 = 12%, rate 2 = 0.85 s^{-1}, amplitude 2 = 88%. Due to the length of data collection for Y167F restacking data appear quantized.

pocket, and prior work suggesting that AdoMet/AdoHcy binding and release are the rate-determining step in the catalytic mechanism (*42*), we sought to explore the role of the water hydrogen bonded to Tyr167 in the M.HhaI catalytic mechanism. The positioning of the water has two potential roles in the methyl-transfer mechanism: (1) In one scenario, as previously postulated (*2*, *16*), the water could contribute to the protonation step envisioned in a concerted reaction mechanism (Scheme 1, step B). (2) Alternatively, the water may stabilize a conformational intermediate prior to or simultaneous with product release (Scheme 1, step C). Taking into account prior knowledge of the mechanism for cytosine methyl transfer (*9*), in particular M.HhaI-catalyzed methyl transfer (*24*), it is unlikely that our newly observed crystallographic water plays a role in nucleophilic attack (Scheme 1, step A). We sought to identify which step(s) in the reaction mechanism rely on this water by mutating Tyr167 to Phe167. This substitution should disrupt the water bonding network by removing a hydrogen-bonding partner between the protein and the water. Our results indirectly show the importance of this water since both the catalytic rate and various thermodynamic constants are altered in the Y167F mutant. Y167F M.HhaI is ~4-fold slower in k_{cat} than WT M.HhaI, yet k_{chem} and $k_{inactivation}$ (Table 1) are unchanged. Single-turnover experiments measuring K_{chem} were performed at 4 °C in order to slow the reaction, hence the reported rate for chemistry being slower than k_{cat} which was measured at 37 °C (Table 1). Measurements of $k_{inactivation}$ are single-turnover experiments with a fluorine atom at the 5 position on the target cytosine which impedes β-elimination and serves as a more sensitive probe for methyl transfer (*8*). Y167F M.HhaI has an ~4-fold tighter affinity for AdoMet than WT and an ~2-fold tighter affinity for DNA (Table 1). Y167F M.HhaI and C81A M.HhaI show similar thermodynamic constants suggesting that when the hydrogen bond between the active site water and Tyr167 is not present, the enzyme is stabilized in a prechemistry complex. Thus, the hydrogen-bonding network involving the active site water and Tyr167 facilitates the transition between prechemistry and postchemistry. However, since removal of the Tyr167 hydroxyl has no effect on the methyl-transfer rate constant, the repositioning of the water molecule must be slowing another step in the reaction mechanism. If a perturbation of the chemistry step was the cause for the 4-fold slower k_{cat}, then the burst magnitude would be severely diminished. However, the retention of a complete burst by Y167F M.HhaI (data not shown) suggests that the product release step(s) is (are) most likely altered by this mutation (Scheme 1, step C).

If the increase in affinity for DNA in the ternary complex is a result of slower release rates, then this should be revealed by slower restacking kinetics of the target base. Indeed, prior structural and functional analysis of M.HhaI has coupled the extrahelical positioning of the target base with increased stability of the ternary complex (*8*, *29*, *30*, *43*). The use of 2-aminopurine (2AP) fluorescence at the position of the target base allows for the monitoring of flipping and restacking kinetics induced by methyltransferases. Although chemistry cannot be performed on 2AP by M.HhaI, 2AP is crystallo-

graphically observed to be flipped into the active site of the enzyme (*26*). Using 2AP as a probe for base flipping, we examined differences in base flipping kinetics between WT and Y167F M.HhaI (Figure 5). A biphasic signal for 2AP flipping was previously assigned to flipping, followed by an isomerization event for the target base (*44*, *45*). Stopped-flow observed decreases in fluorescence with the WT ternary complex were best fit to a double exponential, as were the forward kinetics, which were previously reported; similar results were obtained with the Y167F M.HhaI ternary complex. The double exponential fit for the Y167F restacking kinetics reveals that both phases are ~3-fold slower than the WT restacking kinetics (Figure 5), consistent with the subtle increase in DNA affinity observed with Y167F M.HhaI. Since the target base in the restacking experiments is a purine instead of a pyrimidine, no chemical modification of the target base is occurring. This also suggests, as does the increase in affinity of Y167F M.HhaI for both DNA and cofactor (Table 1), that the altered step in the reaction mechanism of Y167F M.HhaI does not involve attack or β-elimination since neither step is sampled in any of the affinity determinations (Scheme 1, steps A and B). Curiously, the rates for restacking of both WT and Y167F are considerably faster than k_{cat}, but it should be noted that M.HhaI affinity for mismatched base pairs is much greater than for the proper cytosine-guanine base pair (*13*). Thus we have restricted our comparison of restacking kinetics between WT and Y167F M.HhaI, but further extrapolation of the restacking kinetics compared to k_{cat} may be misleading. The combined decrease in k_{cat}, K_D^{AdoMet}, and K_D^{DNA}, slower restacking kinetics, and lack of any change in the methyl-transfer kinetics (Table 1) suggest that the decrease in k_{cat} of Y167F M.HhaI occurs from a slower product release step (Scheme 1, step C). Previous studies have implicated AdoHcy release as the rate-determining step (*42*). Moreover, previously characterized V306A M.HhaI (~2.7 Å from newly identified water) also has an increased affinity for AdoMet (*36*), further validating the coupling between cofactor occupancy and the local molecular structure. Coupled to the proper positioning of the cofactor is closure of the catalytic loop (Figure 1) (*7*, *12*). An alternative hypothesis for the importance of the water positioning is that it assists in loop closure. Thus the product release step in Scheme 1 could be dictated by catalytic loop opening. Since both cofactor positioning and loop closure are coupled, whether the water is important for loop closure or cofactor release is somewhat semantic.

The observed water repositioning corresponding with the occupancy of AdoMet (prechemistry) vs AdoHcy (postchemistry) (Figure 3), in combination with the increase in the product release step observed with the Tyr167 to Phe167 change (Table 1), connects the active site water positioning with cofactor release. Water positioning has previously been implicated to be a contributing factor in the active site dynamics for M.HhaI during catalysis (*16*). Indeed, the water that was implicated by the previous molecular dynamic simulations is important for catalysis, but our work suggests this is due in part to its ability to assist in product release. Disruption of the enzyme hydrogen bonding to the water network hinders the rate of catalysis by stabilizing the ground state energetics of the enzyme−DNA−AdoMet complex.

CONCLUSION

A full mechanistic description of enzyme catalysis requires an understanding of the relevant intermediates leading to rate enhancements. Thus, an important goal is to characterize such intermediates and their interconversion. Presently missing from our understanding of AdoMet-dependent methyl-transfer mechanisms are structural views of precatalytic intermediates in which the substrate and AdoMet are positioned for catalysis. In particular, the positioning of the unmethylated substrate (DNA) and AdoMet immediately prior to catalysis in the DNA cytosine methyl-transfer reaction has not been described. Prior M.HhaI/DNA structures relied exclusively on the use of AdoHcy; here we described the cocrystal structures of several complexes, which provide insights into these intermediates, and show the importance of active site waters in the catalytic mechanism.

Previous studies on M.HhaI reaction intermediates focused on the active site and implicated a water network in the catalytic process of methyl transfer (*16*). These molecular dynamic simulations describe a precatalytic active site which has the target base in the active site pocket of M.HhaI tilted toward the active site nucleophile Cys81 (*16*). Our structural analysis of C81A M.HhaI-DNA-AdoMet, which was designed to reveal atomistic detail of the prechemistry active site, supports this conformational orientation of the target base. Furthermore, this prechemistry intermediate supports the idea that AdoMet-dependent methyl transfer is enhanced by a compression of active site reactants toward each other.

The structural and functional analysis presented here provides support for the use of molecular dynamics simulation to investigate structural conformations as the enzyme transitions from one reaction intermediate to another. Our work also provides new insights into the role of active site waters and cofactor placement in the ternary complex. Our investigation has revealed that indeed the rate-determining step in the catalytic mechanism is product release and that the correct positioning of the active site water assists in release of the cofactor AdoHcy.

ACKNOWLEDGMENT

We thank Dr. John Perona for helpful discussions. We also thank Dr. Steven Jordan and Christopher Mohr for use of the X-ray facility and data processing at Amgen Inc.

REFERENCES

1. Cheng, X., and Roberts, R. J. (2001) AdoMet-dependent methylation, DNA methyltransferases and base flipping, *Nucleic Acids Res. 29*, 3784−3795.
2. Jeltsch, A. (2002) Beyond Watson and Crick: DNA methylation and molecular enzymology of DNA methyltransferases, *ChemBioChem 3*, 274−293.
3. Robertson, K. D., and Wolffe, A. P. (2000) DNA methylation in health and disease, *Nat. Rev. Genet. 1*, 11−19.
4. Heithoff, D. M., Sinsheimer, R. L., Low, D. A., and Mahan, M. J. (1999) An essential role for DNA adenine methylation in bacterial virulence, *Science 284*, 967−970.
5. Mashhoon, N., Carroll, M., Pruss, C., Eberhard, J., Ishikawa, S., Estabrook, R. A., and Reich, N. (2004) Functional characterization of *Escherichia coli* DNA adenine methyltransferase, a novel target for antibiotics, *J. Biol. Chem. 279*, 52075-52081.
6. Jones, P. A. (2003) Epigenetics in carcinogenesis and cancer prevention, *Ann. N.Y. Acad. Sci. 983*, 213−219.

7. Klimasauskas, S., Kumar, S., Roberts, R. J., and Cheng, X. (1994) HhaI methyltransferase flips its target base out of the DNA helix, *Cell 76*, 357−369.
8. Estabrook, R. A., Lipson, R., Hopkins, B., and Reich, N. (2004) The coupling of tight DNA binding and base flipping: identification of a conserved structural motif in base flipping enzymes, *J. Biol. Chem. 279*, 31419−31428.
9. Takusagawa, F., Fujioka, M., Spies, A., and Schowen, R. L. (1998) *S-Adenosylmethionine (AdoMet) Dependent Methyltransferases. Comprehensive Biological Catalysis*, pp 1−30, Book Chapter.
10. Wu, J. C., and Santi, D. V. (1987) Kinetic and catalytic mechanism of HhaI methyltransferase, *J. Biol. Chem. 262*, 4778−4786.
11. Ho, D. K., Wu, J. C., Santi, D. V., and Floss, H. G. (1991) Stereochemical studies of the C-methylation of deoxycytidine catalyzed by HhaI methylase and the N-methylation of deoxyadenosine catalyzed by EcoRI methylase, *Arch. Biochem. Biophys. 284*, 264−269.
12. Cheng, X., Kumar, S., Klimasauskas, S., and Roberts, R. J. (1993) Crystal structure of the HhaI DNA methyltransferase, *Cold Spring Harbor Symp. Quant. Biol. 58*, 331−338.
13. Klimasauskas, S., and Roberts, R. J. (1995) M.HhaI binds tightly to substrates containing mismatches at the target base, *Nucleic Acids Res. 23*, 1388−1395.
14. Kumar, S., Horton, J. R., Jones, G. D., Walker, R. T., Roberts, R. J., and Cheng, X. (1997) DNA containing 4′-thio-2′-deoxycytidine inhibits methylation by HhaI methyltransferase, *Nucleic Acids Res. 25*, 2773−2783.
15. Klimasauskas, S., Szyperski, T., Serva, S., and Wuthrich, K. (1998) Dynamic modes of the flipped-out cytosine during HhaI methyltransferase-DNA interactions in solution, *EMBO J. 17*, 317−324.
16. Lau, E. Y., and Bruice, T. C. (1999) Active site dynamics of the HhaI methyltransferase: insights from computer simulation, *J. Mol. Biol. 293*, 9−18.
17. Lindstrom, W. M., Jr., Flynn, J., and Reich, N. O. (2000) Reconciling structure and function in HhaI DNA cytosine-C-5 methyltransferase, *J. Biol. Chem. 275*, 4912−4919.
18. Vilkaitis, G., Dong, A., Weinhold, E., Cheng, X., and Klimasauskas, S. (2000) Functional roles of the conserved threonine 250 in the target recognition domain of HhaI DNA methyltransferase, *J. Biol. Chem. 275*, 38722−38730.
19. Svedruzic, Z. M., and Reich, N. O. (2004) The mechanism of target base attack in DNA cytosine carbon 5 methylation, *Biochemistry 43*, 11460−11473.
20. Huang, N., and MacKerell, A. D., Jr. (2005) Specificity in protein-DNA interactions: energetic recognition by the (cytosine-C5)-methyltransferase from HhaI, *J. Mol. Biol. 345*, 265−274.
21. Luo, J., and Bruice, T. C. (2005) Low-frequency normal mode in DNA HhaI methyltransferase and motions of residues involved in the base flipping, *Proc. Natl. Acad. Sci. U.S.A. 102*, 16194−16198.
22. Shieh, F. K., Youngblood, B., and Reich, N. O. (2006) The role of Arg165 towards base flipping, base stabilization and catalysis in M.HhaI, *J. Mol. Biol. 362*, 516−527.
23. Mi, S., and Roberts, R. J. (1993) The DNA binding affinity of HhaI methylase is increased by a single amino acid substitution in the catalytic center, *Nucleic Acids Res. 21*, 2459−2464.
24. Zhang, X., and Bruice, T. C. (2006) The mechanism of M.HhaI DNA C5 cytosine methyltransferase enzyme: a quantum mechanics/molecular mechanics approach, *Proc. Natl. Acad. Sci. U.S.A. 103*, 6148−6153.
25. Horton, J. R., Ratner, G., Banavali, N. K., Huang, N., Choi, Y., Maier, M. A., Marquez, V. E., MacKerell, A. D., Jr., and Cheng, X. (2004) Caught in the act: visualization of an intermediate in the DNA base-flipping pathway induced by HhaI methyltransferase, *Nucleic Acids Res. 32*, 3877−3886.
26. Neely, R. K., Daujotyte, D., Grazulis, S., Magennis, S. W., Dryden, D. T., Klimasauskas, S., and Jones, A. C. (2005) Time-resolved fluorescence of 2-aminopurine as a probe of base flipping in M.HhaI-DNA complexes, *Nucleic Acids Res. 33*, 6953−6960.
27. O'Gara, M., Klimasauskas, S., Roberts, R. J., and Cheng, X. (1996) Enzymatic C5-cytosine methylation of DNA: mechanistic implications of new crystal structures for HhaL methyltransferase-DNA-AdoHcy complexes, *J. Mol. Biol. 261*, 634−645.
28. O'Gara, M., Roberts, R. J., and Cheng, X. (1996) A structural basis for the preferential binding of hemimethylated DNA by HhaI DNA methyltransferase, *J. Mol. Biol. 263*, 597−606.
29. O'Gara, M., Horton, J. R., Roberts, R. J., and Cheng, X. (1998) Structures of HhaI methyltransferase complexed with substrates containing mismatches at the target base, *Nat. Struct. Biol. 5*, 872−877.
30. O'Gara, M., Zhang, X., Roberts, R. J., and Cheng, X. (1999) Structure of a binary complex of HhaI methyltransferase with *S*-adenosyl-L-methionine formed in the presence of a short non-specific DNA oligonucleotide, *J. Mol. Biol. 287*, 201−209.
31. Sheikhnejad, G., Brank, A., Christman, J. K., Goddard, A., Alvarez, E., Ford, H., Jr., Marquez, V. E., Marasco, C. J., Sufrin, J. R., O'Gara, M., and Cheng, X. (1999) Mechanism of inhibition of DNA (cytosine C5)-methyltransferases by oligodeoxyribonucleotides containing 5,6-dihydro-5-azacytosine, *J. Mol. Biol. 285*, 2021−2034.
32. Youngblood, B., Shieh, F. K., De Los, Rios S., Perona, J. J., and Reich, N. O. (2006) Engineered extrahelical base destabilization enhances sequence discrimination of DNA methyltransferase M.HhaI, *J. Mol. Biol. 362*, 334−346.
33. Zhou, L., Cheng, X., Connolly, B. A., Dickman, M. J., Hurd, P. J., and Hornby, D. P. (2002) Zebularine: a novel DNA methylation inhibitor that forms a covalent complex with DNA methyltransferases, *J. Mol. Biol. 321*, 591−599.
34. Bruice, T. C., and Bruice, P. Y. (2005) Covalent intermediates and enzyme proficiency, *J. Am. Chem. Soc. 127*, 12478−12479.
35. Bruice, T. C. (2006) Computational approaches: reaction trajectories, structures, and atomic motions. Enzyme reactions and proficiency, *Chem. Rev. 106*, 3119−3139.
36. Sharma, V., Youngblood, B., and Reich, N. (2005) Residues distal from the active site that alter enzyme function in M.HhaI DNA cytosine methyltransferase, *J. Biomol. Struct. Dyn. 22*, 533−544.
37. Marti, S., Roca, M., Andres, J., Moliner, V., Silla, E., Tunon, I., and Bertran, J. (2004) Theoretical insights in enzyme catalysis, *Chem. Soc. Rev. 33*, 98−107.
38. Roca, M., Andres, J., Moliner, V., Tunon, I., and Bertran, J. (2005) On the nature of the transition state in catechol *O*-methyltransferase. A complementary study based on molecular dynamics and potential energy surface explorations, *J. Am. Chem. Soc. 127*, 10648−10655.
39. Ruggiero, G. D., Williams, I. H., Roca, M., Moliner, V., and Tunon, I. (2004) QM/MM determination of kinetic isotope effects for COMT-catalyzed methyl transfer does not support compression hypothesis, *J. Am. Chem. Soc. 126*, 8634−8635.
40. Hoffman, J. L. (1986) Chromatographic analysis of the chiral and covalent instability of *S*-adenosyl-L-methionine, *Biochemistry 25*, 4444−4449.
41. Rhodes, G. (2000) *Crystallography Made Crystal Clear*, 2nd ed., Academic Press, San Diego.
42. Merkiene, E., and Klimasauskas, S. (2005) Probing a rate-limiting step by mutational perturbation of AdoMet binding in the HhaI methyltransferase, *Nucleic Acids Res. 33*, 307−315.
43. Estabrook, R. A., and Reich, N. O. (2006) Observing an induced fit mechanism during sequence specific DNA methylation, *J. Biol. Chem.* (in press).
44. Daujotyte, D., Serva, S., Vilkaitis, G., Merkiene, E., Venclovas, C., and Klimasauskas, S. (2004) HhaI DNA methyltransferase uses the protruding Gln237 for active flipping of its target cytosine, *Structure (Cambridge) 12*, 1047−1055.
45. Allan, B. W., Beechem, J. M., Lindstrom, W. M., and Reich, N. O. (1998) Direct real time observation of base flipping by the EcoRI DNA methyltransferase, *J. Biol. Chem. 273*, 2368−2373.
46. Jones, T. A., Zou, J. Y., Cowan, S. W., and Kjeldgaard (1991) Improved methods for building protein models in electron density maps and the location of errors in these models, *Acta Crystallogr. A47* (Part 2), 110−119.
47. Brunger, A. T., Adams, P. D., Clore, G. M., DeLano, W. L., Gros, P., Grosse-Kunstleve, R. W., Jiang, J. S., Kuszewski, J., Nilges, M., Pannu, N. S., Read, R. J., Rice, L. M., Simonson, T., and Warren, G. L. (1998) Crystallography & NMR system: A new software suite for macromolecular structure determination, *Acta Crystallogr., Sect. D: Biol. Crystallogr. 54*, 905−921.
48. Allan, B. W., and Reich, N. O. (1996) Targeted base stacking disruption by the EcoRI DNA methyltransferase, *Biochemistry 35*, 14757−14762.

BI7005948